Spin-echo, Fidelity and the Quantum Critical Fan in $TmVO_4$

Y-H. Nian,[1] I. Vinograd,[1] T. Green,[1] C. Chaffey,[1] P. Massat,[2]
R. R. P. Singh,[1] M. P. Zic,[3] I. R. Fisher,[2] and N. J. Curro[1,*]

[1] *Department of Physics and Astronomy, University of California Davis, Davis, CA*
[2] *Geballe Laboratory for Advanced Materials and Department of Applied Physics, Stanford University, CA 94305, USA*
[3] *Geballe Laboratory for Advanced Materials and Department of Physics, Stanford University, CA 94305, USA*

(Dated: April 23, 2024)

Using spin-echo Nuclear Magnetic Resonance in the model Transverse-Field Ising system $TmVO_4$, we show that low frequency quantum fluctuations at the quantum critical point have a very different effect on ^{51}V nuclear-spins than classical low-frequency noise or fluctuations that arise at a finite temperature critical point. Spin-echos filter out the low frequency classical noise but not the quantum fluctuations. This allows us to directly visualize the quantum critical fan and demonstrate the persistence of quantum fluctuations at the critical coupling strength in $TmVO_4$ to high temperatures in an experiment that remains transparent to finite temperature classical phase transitions. These results show that while dynamical decoupling schemes can be quite effective in eliminating classical noise in a qubit, a quantum critical environment may lead to rapid entanglement and decoherence.

Unconventional superconductivity tends to emerge in materials in the vicinity of a quantum phase transition [1–9], however disentangling competing order parameters and the effects of disorder challenge our ability to discern what interactions or effective Hamiltonians drive the essential physics of these materials. In order to make progress, it is valuable to investigate paradigmatic systems with parameters that can be well controlled. A prominent example is $LiHoF_4$, a ferromagnet whose behavior is captured by the transverse field Ising model (TFIM) [10].

Recently, $TmVO_4$ has emerged as another model TFIM system, with novel features. It has a ferro-quadrupolar order parameter, which is even under time reversal symmetry and hence cannot couple to fields that are odd under time-reversal, such as an external magnetic field or nuclear spin. However, a transverse component of the order parameter is dipolar and couples to a magnetic field along the crystalline c-axis [11] leading to a realization of a transverse-field Ising model. The electric quadrupolar moments of the Tm 4f orbitals couple strongly to the lattice strain, giving rise to long-range order through a cooperative Jahn-Teller effect [12]. The effective Hamiltonian can be described by coupled quadrupolar Ising spins with B_{2g} symmetry, whereas both B_{1g} strain and c-axis magnetic fields act as transverse fields [13].

The distinguishing property of a quantum critical point is that there are large quantum fluctuations of the order parameter at $T = 0$ over all length and time scales [14–16]. These fluctuations persist to higher temperatures over a range of parameter space, giving rise to a 'quantum critical fan' in the phase diagram. The fluctuations affect bulk properties such as resistivity, susceptibility and specific heat, enabling detailed maps of the quantum critical fan to be inferred from the temperature dependence of these quantities [17–21]. The presence of such fluctuations can also be inferred from the temperature dependence of the dynamical susceptibility, which can exhibit E/T scaling in the vicinity of the QCP [22–24].

Quantum fluctuations arise due to the presence of competing terms in the Hamiltonian that do no commute (e.g., the transverse field versus the Ising interaction), and their dynamics are driven by the intrinsic properties of the Hamiltonian. Thermal fluctuations, in contrast, are driven by the wide range of states explored in a statistical ensemble at finite temperatures, with low frequency fluctuations that are controlled via extrinsic parameters. Both incoherent thermal and coherent quantum fluctuations contribute to the noise fluctuation spectrum at finite temperature. Away from the quantum critical coupling, however, quantum fluctuations remain at high frequency while classical fluctuations become soft at phase transitions [25]. We demonstrate that this distinction enables us to uniquely probe the quantum critical fluctuations in $TmVO_4$ using nuclear magnetic resonance (NMR) spin echoes, thus revealing a clear map of the quantum critical fan in this material.

Several years ago the quantum information community considered the question of how a qubit coupled to a noisy environment undergoes decoherence. To model such behavior, they considered a specific type of coupling to a transverse field Ising model as it is tuned through a quantum phase transition [26–28]. This model proved fruitful theoretically, but had never been tested experimentally. $TmVO_4$ offers a unique opportunity to study this problem experimentally, because the non-Kramers doublet ground state of $TmVO_4$ ensures that hyperfine interaction between the nuclear spin (I_x) and the Ising operator corresponding to the transverse field direction (σ_x) has exactly the same form as the theoretical models: $I_x\sigma_x$ [29]. Moreover, this coupling means that the NMR relaxation is controlled by the transverse susceptibility exclusively, without any contamination from the longitudinal degrees of freedom which normally dominate the behavior near a QCP.

Distinguishing classical and quantum fluctuations at finite temperatures is a problem of fundamental interest in many-body physics and quantum information [30–33]. Our results demonstrate a key distinction in the effect a quantum critical environment has on decoherence of a qubit compared with classical sources of low frequency noise [25–28]. While classical noise can be filtered out by spin-echo and other dynamical decoupling schemes, coupling to a quantum critical environment leads to a qubit's rapid entanglement and decoherence.

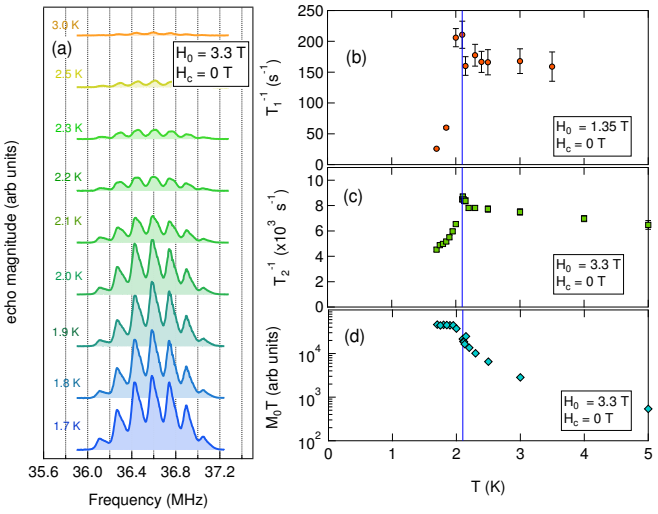

FIG. 1. (a) ^{51}V NMR spectra for $H_c = 0$ as a function of temperature. The spectra have been offset vertically for clarity. Panels (b,c,d) show the spin-lattice relaxation rate, T_1^{-1}, the decoherence rate T_2^{-1}, and the magnitude of the echo decay envelope times temperature as a function of temperature. All measurements were conducted with the applied field oriented perpendicular to (001). The vertical blue line indicates T_Q.

Spin Echo Intensity- Fig. 1(a) shows ^{51}V NMR spectra for a series of temperatures crossing the ferroquadrupolar transition at $H_c = 0$ (with the applied field in the ab plane). The spectra reveal seven peaks split by the nuclear quadrupolar interaction, but no discernable change in the overall shift or the quadrupolar splitting between the peaks. Both the spin lattice relaxation rate, T_1^{-1}, and the spin echo decoherence rate, T_2^{-1}, shown in panels (b) and (c), exhibit small peaks at T_Q, but are suppressed in the ordered state, and the magnitude of the echo decay envelope, M_0T (d), shows no change through the phase transition. These results are consistent with previous measurements at low fields [34].

The NMR response when crossing the phase transition as a function of the transverse field at constant temperature is dramatically different. Fig. 2 shows how the spectra evolve as the field $\mathbf{H}_0$ is rotated in the (010) plane at $T = 1.7$ K. Here, the c-axis projection, $H_c = H_0 \cos\theta$, where θ is the angle relative to the [001] direction (see inset of Fig. 2(a)). The seven peaks in the spectrum shift

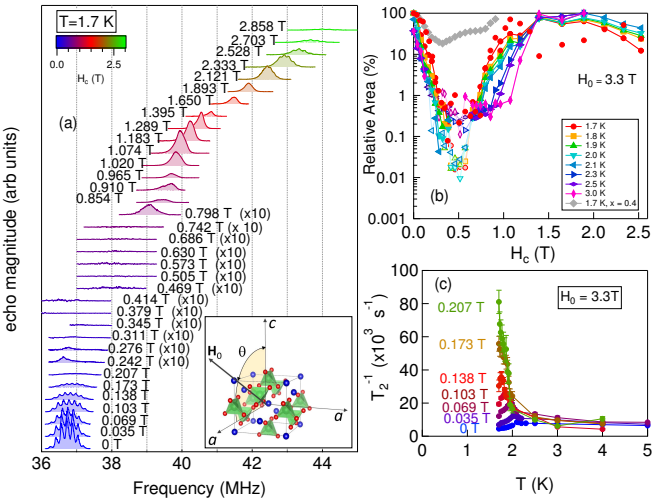

FIG. 2. (a) ^{51}V NMR spectra at 1.7 K as a function of field along the c-axis, $H_c = H_0 \cos\theta$ where $H_0 = 3.3$ T. The field is rotated in the (010) plane. The spectra have been offset vertically for clarity, and have been normalized by the number of scans. Spectra between 0.242 - 0.798 T have been multiplied by a factor of ten. The inset shows the $TmVO_4$ unit cell, with Tm (blue), V (green), and O (red) atoms, and the orientation of the field. (b) Integrated spectral area normalized by their values at 1.5 T as a function of transverse field at various temperatures for $H_0 = 3.3$ T. The gray points correspond to $Tm_{0.6}Y_{0.4}VO_4$. The light colored points correspond to longer delay times [35]. (c) Decoherence rate, T_2^{-1} versus temperature for several different values of H_c.

upwards in frequency and closer together as H_c increases. This behavior is well-described by the anisotropic Knight shift and electric field gradient tensors [36]. Surprisingly, the integrated spectral area is greatly reduced (wipeout) for a range of fields in the vicinity of $H_c^* = 0.5$ T. This quantity is shown in panel (b) for a series of temperatures, and exhibits a drop of approximately four orders of magnitude near H_c^*. The wipeout effect is well known from the study of the cuprates and arises due to a dramatic increase in the distribution of spin decoherence rates, T_2^{-1} [37–41]. An important difference, however, is that in $TmVO_4$ the effect occurs in a homogeneous system, without the presence of any dopants. The spectra are obtained by measuring the size of the spin echo as a function of frequency for a fixed pulse spacing, τ, and the echo size is proportional to $\exp[-2\tau/T_2]$. The intensity decreases, and because the spectrometer cannot operate for arbitrarily small τ, the echo intensity will vanish for sufficiently large T_2^{-1}. This interpretation is supported by direct measurements of T_2^{-1} for small H_c, shown in panel (c) for fields up to 0.2 T. Beyond this field it is not possible to obtain a direct measurement due to the wipeout effect.

This wipeout of the NMR signal persists to higher temperatures, as shown in Fig. 2(b). In this case, the spectra are integrated as a function of frequency, and normalized

by the value at 1.5 T at each temperature. The wipeout effect in the vicinity of H_c^* persists up to temperatures well above the ordering temperature $T_Q = 2.15$ K. Moreover, the range of fields throughout which the signal experiences wipeout broadens with temperature, giving rise to a fan-shaped region emerging from the quantum critical point, as illustrated in Fig. 3(a). We approximate the quantum critical - quantum disordered crossover temperature as the point where the relative area is 5%, shown as green circles in the figure. The dashed line is a fit to $(H_c - H_c^*)^\beta$, where $\beta = 0.75 \pm 0.06$.

In order to check whether this wipeout is related to the QCP, we also measured the signal in $Tm_{0.6}Y_{0.4}VO_4$. Long range ferroquadrupolar order vanishes in the Y-doped material beyond a critical doping level of ~ 0.2. The intensity versus H_c data for this compound, shown as gray points in Fig. 2(a), exhibits a slight reduction, but the effect is much less than that observed in the pure $TmVO_4$. These results point to quantum critical fluctuations as a mechanism for the signal wipeout in this material.

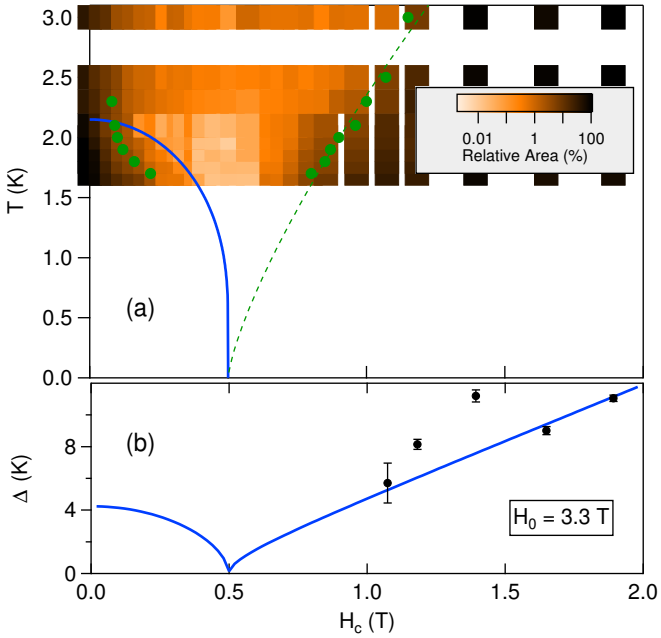

FIG. 3. (a) Phase diagram, with measured points colored by relative area of the spectra intensity. The solid blue line is the ferroquadrupolar ordering temperature, $T_Q(H_c)$, reproduced from [11]. The green circles correspond to the points where the relative signal area is 5%, and the dashed line is a fit as described in the text. (b) The calculated gap, Δ (solid line), and the measured gap (•) extracted from fits to the T_1^{-1}, as described in the text. $\Delta(H_c = 0)$ is set to 4.2 K as reported in [42].

For sufficiently large H_c, the signal intensity recovers and it is possible to directly measure T_1^{-1}. Figs. 4(a,b) show how this quantity varies as a function of temperature and field. In this range, we find that T_1^{-1} exhibits activated behavior, $T_1^{-1} \propto \exp[-\Delta/T]$. The gap, Δ, is shown as a function of H_c in Fig. 3(b) (•), and agrees well with numerical calculations (solid line) [43] .

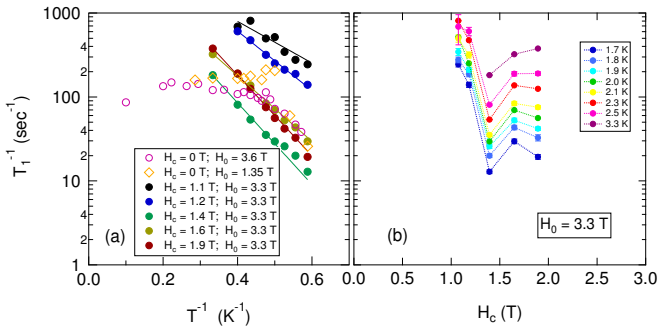

FIG. 4. The spin lattice relaxation rate of the ^{51}V as a function of inverse temperature (a) and field (b). The solid lines are fits to an activated behavior, as discussed in the text. The open data points for $H_c = 0$ are reproduced from [34] for the magnetic relaxation channel.

Decoherence and Quantum Criticality.- The Tm ground state doublets are described by the Hamiltonian:

$$\mathcal{H} = -J \sum_{i,j \in n.n.} \hat{\sigma}_z(i)\hat{\sigma}_z(j) + \lambda \sum_i \hat{\sigma}_x(i) \qquad (1)$$

where $\sigma_z(i)$ is the B_{2g} quadrupolar moment of the Tm at site i, σ_x is the spin moment of the Tm along the c-axis, J is the ferroquadrupolar exchange coupling, $\lambda = g_c \mu_B H_c$, and $g_c = 10$ for $TmVO_4$ [13]. The coupling to the nuclei is given by the hyperfine interaction: $\mathcal{H}_{hyp} = A_{cc} \sum_i I_x(i)\sigma_x(i)$, where $A_{cc}/J \approx 2 \times 10^{-4}$ and $I_x(i)$ is the nuclear spin along the c-axis [29, 35]. A similar problem was investigated for the case of a single central spin coupled to a 1D ring of Ising variables at $T = 0$ in order to investigate the decoherence of the central spin state as a consequence of its coupling to a quantum critical environment [26]. In that case, a pure state of the central spin quickly entangles with the environment forming a mixed state, and the decoherence rate reaches a maximum at the QCP. This model can be generalized to capture the relevant physics of the ^{51}V NMR signal in $TmVO_4$, in which there is a nuclear spin located at each lattice site [35]. The NMR free induction decay (FID) amplitude can be expressed as: $L_{FID}(t) = |\langle\phi_g(t)|\phi_e(t)\rangle|$, where $|\phi_{e,g}(t)\rangle = \exp(-i\mathcal{H}_{e,g}t)|\phi(0)\rangle$ and $\mathcal{H}_{g,e} = \mathcal{H} \pm A_{cc}\sigma_x/2$. In other words, the FID is measure of the fidelity between two states that evolve from an initial state, $|\phi(0)\rangle$, under slightly different Hamiltonians in which the transverse field is either $H_c \pm A_{cc}/2g_c\mu_B$. Note that if $\mathcal{H}_{hyp}$ includes terms coupling to σ_z, then the NMR response is no longer a simple function of the fidelity. In a spin echo experiment, the nuclear spins are refocused with a 180° pulse at time τ, and the echo forms at time 2τ with amplitude $L_{echo}(2\tau) = |\langle\phi_{ge}(2\tau)|\phi_{eg}(2\tau)\rangle|$ where $|\phi_{eg,ge}(2\tau)\rangle = \exp(-i\mathcal{H}_{g,e}\tau)\exp(-i\mathcal{H}_{e,g}\tau)|\phi(0)\rangle$. If the

system is far from the QCP then a slightly different transverse field will not significantly affect the time evolution of the state and the fidelity will decay slowly. However, close to the QCP, where the fidelity susceptibility is largest, a small change of the transverse field can dramatically alter the wavefunction and the fidelity will rapidly decay with time.

At finite temperatures, the electronic wavefunction is no longer in a pure state and thermally excited states with different local fields will interact with the nuclei. Both quantum fluctuations driven by the intrinsic dynamics of the system as well as incoherent thermal fluctuations will contribute to the decoherence of the FID signal, washing out the enhancement at the QCP. On the other hand, in a spin echo experiment the refocusing pulse dynamically decouples low frequency fluctuations [44]. Chen *et al.* showed that the spin echo remains sensitive to the quantum critical fluctuations even at high temperatures in the 1D transverse field Ising model [28]. Our results shown in Figs. 1(b) and 3 confirm this interpretation. The spin echo intensity is suppressed by quantum critical fluctuations to temperatures above T_Q.

The NMR decoherence rate reflects an enhanced fidelity susceptibility, which can be related to the dynamical structure factor [45]:

$$S_{xx}(\omega) = \int_0^\infty \langle \sigma_x(\tau)\sigma_x(0)\rangle e^{i\omega\tau} d\tau. \qquad (2)$$

The fluctuations $\langle \delta^2\sigma_x\rangle = \langle \sigma_x^2\rangle - \langle \sigma_x\rangle^2$ can be written as the sum of a thermal contribution $\langle \delta^2\sigma_x\rangle_T$ and a quantum contribution $\langle \delta^2\sigma_x\rangle_Q$ [25]. The incoherent thermal fluctuations are related to the transverse field susceptibility, χ_x, via the classical fluctuation-dissipation theorem: $\langle \delta^2\sigma_x\rangle_T = \chi_x k_B T$. These thermal fluctuations contribute primarily to the low frequency behavior of $S_{xx}(\omega)$. Coherent quantum fluctuations contribute to $S_{xx}(\omega)$ at finite frequency, away from the quantum critical point. The decoherence of an FID can also be derived via Bloch-Wangsness-Redfield theory, which predicts an exponential decay $L_{FID} \sim e^{-t/T_2}$ where $T_2^{-1} = A_{cc}^2 S_{xx}(0)/2\hbar^2$ [46–48]. For a spin echo, however, $L_{echo}(2\tau)$ can be expressed as a convolution of $S_{xx}(\omega)$ with a filter function, $F(\omega\tau)$ that encapsulates the influence of the 180° refocusing pulse [44]. In this case contributions of $S_{xx}(\omega)$ at frequencies $\omega \ll 1/\tau \approx 10^5$ Hz are filtered out. As a result, contributions from thermal fluctuations are removed from the spin echo decoherence rate, but not quantum fluctuations at higher frequencies [28, 49]. This distinction explains not only why the V signal intensity is able to map out the quantum critical fan but also why T_2^{-1} changes little across the thermal phase transition at $H_c = 0$ in Fig. 1(c), where there are little to no quantum fluctuations.

In mean-field theory, the static transverse susceptibility decreases monotonically with field as $(\mathrm{sech}\,(\lambda/T))^2/T$ in the paramagnetic phase, which at low temperatures has the activated form $\frac{1}{T}\exp(-\Delta/T)$ consistent with the excitation gap $\Delta = 2\lambda$. In contrast, for the 3-dimensional TFIM [43] the $T = 0$ transverse-susceptibility is known to diverge logarithmically as one approaches the QCP from *either* side of the transition [50, 51]. At the finite temperature transition the transverse susceptibility should diverge with the specific heat exponent $\alpha \approx 0.1$ for a 3-dimensional Ising model. However, our quadrupolar system differs from a spin model in that the coupling of the order parameter to the lattice leads to long-range interactions, especially near the transition where phonons become soft [52–54], leading to mean-field behavior. This may cause a finite jump in transverse susceptibility at the transition. Behavior of the transverse susceptibility in such systems deserves further theoretical attention. Nevertheless, one expects the gap to go to zero at the quantum critical point.

A recent theoretical study of the 1D TFIM also predicted that $S_{xx}(\omega)$ should exhibit thermally activated behavior at low frequencies: $S_{xx} \sim \exp[-\Delta/T]$ for $\omega \ll T \ll \Delta$, where Δ is the excitation gap in the quantum disordered regime [55]. We therefore postulate that the NMR intensity can be described both in the disordered and the ordered states as:

$$I(T, H_c) = I_0 \exp[-\alpha e^{-\Delta(H_c)/T}/T] \qquad (3)$$

where $\alpha \sim \tau A_{cc}^2$ is a constant. The functional form of $\Delta(H_c)$ has been computed as a function of transverse field for different 3D cubic lattices [43], and is constrained by the measured value of $\Delta(0) = 4.24$ K in the limit $H_c \ll H_c^*$ [42]. For $H_c \gg H_c^*$, Δ approaches $g_c\mu_B H_c$, the single ion gap for the ground state doublet [12, 56]. This function is shown in Fig. 3(b). We fit the intensity data at 1.7 K to Eq. 3, as shown in Fig. 5. The intensity is normalized by the value at $H_c = 1.5$ T for each temperature, and the only variable parameter is α. There is excellent agreement, and the increasing width as a function of temperature agrees with the observed trend seen in Figs. 2(b) and 3(a). The fit is less good for low H_c, and we speculate that this behavior may reflect the fact that there remains a finite field $H_0 \sin\theta$ in the longitudinal direction in this limit. The Ising variables couple to this field to second order [34], which may give rise to higher order effects not captured by the fitting function.

The gap extracted from T_1^{-1} measurements compares well with the expected values of $\Delta(H_c)$ as shown in Fig. 3(b), however it has been argued that $T_1^{-1} \sim \exp[-2\Delta/T]$ [55]. This result was based on the assumption of a hyperfine interaction that includes a coupling to $S_{zz}(\omega)$, the structure function for longitudinal fields. Such a coupling is absent in $TmVO_4$, but spin lattice relaxation is driven by fluctuations perpendicular to the quantization axis, $\mathbf{H}_0$, which is not parallel to the transverse field in our case. Therefore, S_{xx} can contribute to T_1^{-1}, and hence we expect $T_1^{-1} \sim \exp[-\Delta/T]$.

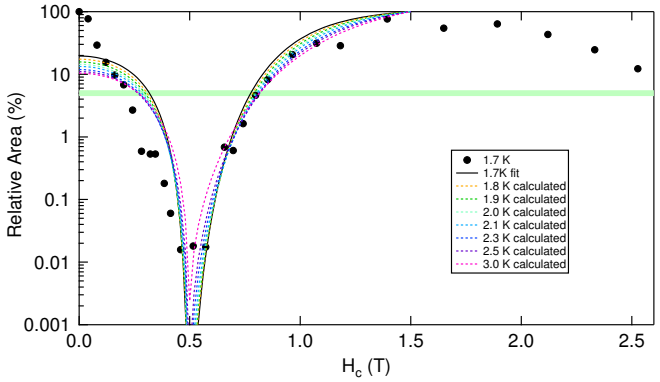

FIG. 5. The relative area (•) at 1.7 K versus transverse field. The solid black line is a fit to Eq. 3 at 1.7 K with $\alpha = 36 \pm 8$, and the dashed colored lines correspond to the same function computed at different temperatures. The horizontal green bar represents the 5% level corresponding to the green data points in Fig. 3(a).

It is noteworthy that both $TmVO_4$ and $LiHoF_4$ are model systems for the 3D TFIM due to the non-Kramers nature of the ground state $4f$ electrons, but an important difference between the two, aside from the nature of the long-range order, is the anisotropy of the hyperfine coupling to the nuclear spin degrees of freedom. In the latter, the ^{165}Ho nuclear spin couples to the 4f magnetic moment along the longitudinal (order-parameter) axis, giving rise to a composite spin at low temperatures which modifies the shape of the phase boundary near the QCP [10]. Consequently a larger transverse field is required in order to fully destroy the ferromagnetic state. In $TmVO_4$, the ^{169}Tm nuclear spin also couples to the 4f magnetic moment, but only along the transverse direction [56].

Conclusions - $TmVO_4$ presents a unique realization of transverse-field Ising model, where the order parameter is even under time reversal symmetry and does not couple to external magnetic fields or nuclear spins, but a transverse component of the order-parameter does. Coupling of the nuclear spin purely to the transverse component allows us to probe the decoherence of the nuclear spin as the electronic system is tuned through a quantum critical point. Our observation of NMR wipeout of the ^{51}V in $TmVO_4$ provides experimental confirmation that a qubit coupled to a quantum critical environment quickly transitions from a pure to a mixed state [26]. It is perhaps natural to expect that such an environment would be detrimental to any application in which the qubits are used as a resource for quantum information. Conversely, these results also suggest that an ensemble of strongly coupled qubits, such as in a spin-based quantum computer, would similarly be sensitive to noise arising from nearby nuclear spins which could limit the coherence time for quantum computations. Our findings may also inspire new ways to think about NMR wipeout effects observed in cuprates, pnictides and other complex systems and their relation to quantum entanglement and fidelity in those systems.

We acknowledge helpful discussions with A. Albrecht, R. Baunach and F. Ronning. Work at UC Davis was supported by the NSF under Grants No. DMR-1807889 and PHY-1852581, as well as the UC Laboratory Fees Research Program ID LFR-20-653926. Crystal growth performed at Stanford University was supported by the Air Force Office of Scientific Research under award number FA9550-20-1-0252. P. M. was partially supported by the Gordon and Betty Moore Foundation Emergent Phenomena in Quantum Systems Initiative through Grant GBMF9068, and M.Z. was partially supported by the NSF under Grant No. DGE-1656518.

REFERENCES

* njcurro@ucdavis.edu

[1] F. F. Balakirev, J. B. Betts, A. Migliori, S. Ono, Y. Ando, and G. S. Boebinger, Signature of optimal doping in Hall-effect measurements on a high-temperature superconductor, Nature **424**, 912 (2003).
[2] P. Coleman and A. J. Schofield, Quantum criticality, Nature **433**, 226 (2005).
[3] T. Park, F. Ronning, H. Q. Yuan, M. B. Salamon, R. Movshovich, J. L. Sarrao, and J. D. Thompson, Hidden magnetism and quantum criticality in the heavy fermion superconductor $CeRhIn_5$, Nature **440**, 65 (2006).
[4] T. Park, V. A. Sidorov, F. Ronning, J.-X. Zhu, Y. Tokiwa, H. Lee, E. D. Bauer, R. Movshovich, J. L. Sarrao, and J. D. Thompson, Isotropic quantum scattering and unconventional superconductivity, Nature **456**, 366 (2008).
[5] T. Shibauchi, A. Carrington, and Y. Matsuda, A quantum critical point lying beneath the superconducting dome in iron pnictides, Annu. Rev. Condens. Matter Phys. **5**, 113 (2014).
[6] H.-H. Kuo, J.-H. Chu, J. C. Palmstrom, S. A. Kivelson, and I. R. Fisher, Ubiquitous signatures of nematic quantum criticality in optimally doped Fe-based superconductors, Science **352**, 958 (2016).
[7] S. Lederer, Y. Schattner, E. Berg, and S. A. Kivelson, Enhancement of superconductivity near a nematic quantum critical point, Phys. Rev. Lett. **114**, 097001 (2015).
[8] E. Schuberth, M. Tippmann, L. Steinke, S. Lausberg, A. Steppke, M. Brando, C. Krellner, C. Geibel, R. Yu, Q. Si, and F. Steglich, Emergence of superconductivity in the canonical heavy-electron metal $YbRh_2Si_2$, Science **351**, 485 (2016).
[9] S. Paschen and Q. Si, Quantum phases driven by strong correlations, Nature Review Physics **3**, 9 (2020).
[10] D. Bitko, T. F. Rosenbaum, and G. Aeppli, Quantum critical behavior for a model magnet, Phys. Rev. Lett. **77**, 940 (1996).

[11] P. Massat, J. Wen, J. M. Jiang, A. T. Hristov, Y. Liu, R. W. Smaha, R. S. Feigelson, Y. S. Lee, R. M. Fernandes, and I. R. Fisher, Field-tuned ferroquadrupolar quantum phase transition in the insulator $TmVO_4$, Proc. Natl. Acad. Sci. **119**, e2119942119 (2022).

[12] G. A. Gehring and K. A. Gehring, Co-operative Jahn-Teller effects, Rep. Prog. Phys. **38**, 1 (1975).

[13] A. V. Maharaj, E. W. Rosenberg, A. T. Hristov, E. Berg, R. M. Fernandes, I. R. Fisher, and S. A. Kivelson, Transverse fields to tune an Ising-nematic quantum phase transition, Proc. Natl. Acad. Sci. **114**, 13430 (2017).

[14] S. Chakravarty, B. I. Halperin, and D. R. Nelson, Two-dimensional quantum heisenberg antiferromagnet at low temperatures, Phys. Rev. B **39**, 2344 (1989).

[15] S. Chakravarty, B. I. Halperin, and D. R. Nelson, Low-temperature behavior of two-dimensional quantum antiferromagnets, Phys. Rev. Lett. **60**, 1057 (1988).

[16] S. Sachdev, *Quantum Phase Transitions* (Cambridge University Press, 2001).

[17] S. Ohsugi, Y. Kitaoka, K. Ishida, and K. Asayama, Cu NQR study of the spin dynamics in high-T_c superconductor $La_{2-x}Sr_xCuO_4$, J. Phys. Soc. Jpn. **60**, 2351 (1991).

[18] J. Custers, P. Gegenwart, H. Wilhelm, K. Neumaier, Y. Tokiwa, O. Trovarelli, C. Geibel, F. Steglich, C. Pepin, and P. Coleman, The break-up of heavy electrons at a quantum critical point, Nature **424**, 524 (2003).

[19] G. R. Stewart, Non-Fermi-liquid behavior in d- and f-electron metals, Rev. Mod. Phys. **73**, 797 (2001).

[20] T. Iye, Y. Nakai, S. Kitagawa, K. Ishida, S. Kasahara, T. Shibauchi, Y. Matsuda, and T. Terashima, Gradual suppression of antiferromagnetism in $BaFe_2(As_{1-x}P_x)_2$: Zero-temperature evidence for a quantum critical point, Phys. Rev. B **85**, 184505 (2012).

[21] J.-H. Chu, H.-H. Kuo, J. G. Analytis, and I. R. Fisher, Divergent nematic susceptibility in an iron arsenide superconductor, Science **337**, 710 (2012).

[22] A. Schroder, G. Aeppli, R. Coldea, M. Adams, O. Stockert, H. Lohneysen, E. Bucher, R. Ramazashvili, and P. Coleman, Onset of antiferromagnetism in heavy-fermion metals, Nature **407**, 351 (2000).

[23] M. Vojta, Quantum phase transitions, Rep. Prog. Phys. **66**, 2069 (2003).

[24] Q. Si and F. Steglich, Heavy fermions and quantum phase transitions, Science **329**, 1161 (2010).

[25] I. Frérot and T. Roscilde, Quantum variance: A measure of quantum coherence and quantum correlations for many-body systems, Phys. Rev. B **94**, 075121 (2016).

[26] H. T. Quan, Z. Song, X. F. Liu, P. Zanardi, and C. P. Sun, Decay of Loschmidt echo enhanced by quantum criticality, Phys. Rev. Lett. **96**, 140604 (2006).

[27] S.-J. Gu, Fidelity approach to quantum phase transitions, Int. J. Mod Phys B **24**, 4371 (2010).

[28] S.-W. Chen, Z.-F. Jiang, and R.-B. Liu, Quantum criticality at high temperature revealed by spin echo, New J. Phys. **15**, 043032 (2013).

[29] S. Washimiya, K. Shinagawa, and S. Sugano, Effective Hamiltonian for non-Kramers doublets, Phys. Rev. B **1**, 2976 (1970).

[30] T.-C. Lu and T. Grover, Singularity in entanglement negativity across finite-temperature phase transitions, Phys. Rev. B **99**, 075157 (2019).

[31] T.-C. Lu and T. Grover, Structure of quantum entanglement at a finite temperature critical point, Phys. Rev. Res. **2**, 043345 (2020).

[32] J. Martyn and B. Swingle, Product spectrum ansatz and the simplicity of thermal states, Phys. Rev. A **100**, 032107 (2019).

[33] N. E. Sherman, T. Devakul, M. B. Hastings, and R. R. P. Singh, Nonzero-temperature entanglement negativity of quantum spin models: Area law, linked cluster expansions, and sudden death, Phys. Rev. E **93**, 022128 (2016).

[34] I. Vinograd, K. R. Shirer, P. Massat, Z. Wang, T. Kissikov, D. Garcia, M. D. Bachmann, M. Horvatić, I. R. Fisher, and N. J. Curro, Second order Zeeman interaction and ferroquadrupolar order in $TmVO_4$, npj Quantum Materials **7**, 68 (2022).

[35] See Supplemental Material [url] for descriptions of sample preparation, spectral structure, hyperfine couplings, and generalization of the central spin model to nuclei in a lattice, which includes Refs. [57-58].

[36] Z. Wang, I. Vinograd, Z. Mei, P. Menegasso, D. Garcia, P. Massat, I. R. Fisher, and N. J. Curro, Anisotropic nematic fluctuations above the ferroquadrupolar transition in $TmVO_4$, Phys. Rev. B **104**, 205137 (2021).

[37] N. Curro and P. Hammel, The Cu NMR echo decay in stripe ordered $La_{1.65}Eu_{0.2}Sr_{0.15}CuO_4$, Phys. C **341**, 1797 (2000).

[38] N. Curro, P. Hammel, B. Suh, M. Hücker, B. Büchner, U. Ammerahl, and A. Revcolevschi, Inhomogeneous low frequency spin dynamics in $La_{1.65}Eu_{0.2}Sr_{0.15}CuO_4$, Phys. Rev. Lett. **85**, 642 (2000).

[39] A. Hunt, P. Singer, K. Thurber, and T. Imai, ^{63}Cu NQR measurement of stripe order parameter in $La_{2-x}Sr_xCuO_4$, Phys. Rev. Lett. **82**, 4300 (1999).

[40] M.-H. Julien, A. Campana, A. Rigamonti, P. Carretta, F. Borsa, P. Kuhns, A. P. Reyes, W. G. Moulton, M. Horvatić, C. Berthier, A. Vietkin, and A. Revcolevschi, Glassy spin freezing and NMR wipeout effect in the high-T_c superconductor $La_{1.90}Sr_{0.10}CuO_4$ critical discussion of the role of stripes, Phys. Rev. B **63**, 144508 (2001).

[41] A. P. Dioguardi, J. Crocker, A. C. Shockley, C. H. Lin, K. R. Shirer, D. M. Nisson, M. M. Lawson, N. apRoberts Warren, P. C. Canfield, S. L. Bud'ko, S. Ran, and N. J. Curro, Coexistence of cluster spin glass and superconductivity in $Ba(Fe_{1-x}Co_x)_2As_2$ for $0.060 \leq x \leq 0.071$, Phys. Rev. Lett. **111**, 207201 (2013).

[42] P. J. Becker, M. J. M. Leask, and R. N. Tyte, Optical study of the cooperative Jahn-Teller transition in thulium vanadate, $TmVO_4$, J. Phys. C: Solid State Phys. **5**, 2027 (1972).

[43] Z. Weihong, J. Oitmaa, and C. J. Hamer, Series expansions for the 3D transverse Ising model at T=0, J. Phys. A: Math. Gen. **27**, 5425 (1994).

[44] Ł. Cywiński, R. M. Lutchyn, C. P. Nave, and S. D. Sarma, How to enhance dephasing time in superconducting qubits, Phys. Rev. B **77**, 174509 (2008).

[45] W.-L. You, Y.-W. Li, and S.-J. Gu, Fidelity, dynamic structure factor, and susceptibility in critical phenomena, Phys. Rev. E **76**, 022101 (2007).

[46] R. K. Wangsness and F. Bloch, The Dynamical Theory of Nuclear Induction, Phys. Rev. **89**, 728 (1953).

[47] A. G. Redfield, On the Theory of Relaxation Processes, IBM J. Res. Dev. **1**, 19 (1957).

[48] C. P. Slichter, *Principles of Nuclear Magnetic Resonance*, 3rd ed. (Springer-Verlag, 1992).

[49] S.-W. Chen and R.-B. Liu, Faraday rotation echo spectroscopy and detection of quantum fluctuations, Scientific Reports **4**, 4695 (2014).

[50] E. Brezin, J. C. Le Guillou, and J. Zinn-Justin, Approach to scaling in renormalized perturbation theory, Phys. Rev. D **8**, 2418 (1973).
[51] F. J. Wegner and E. K. Riedel, Logarithmic corrections to the molecular-field behavior of critical and tricritical systems, Phys. Rev. B **7**, 248 (1973).
[52] U. Karahasanovic and J. Schmalian, Elastic coupling and spin-driven nematicity in iron-based superconductors, Phys. Rev. B **93**, 064520 (2016).
[53] I. Paul and M. Garst, Lattice effects on nematic quantum criticality in metals, Phys. Rev. Lett. **118**, 227601 (2017).
[54] Y. Qi and C. Xu, Global phase diagram for magnetism and lattice distortion of iron-pnictide materials, Phys. Rev. B **80**, 094402 (2009).
[55] J. Yang, W. Yuan, T. Imai, Q. Si, J. Wu, and M. Kormos, Local dynamics and thermal activation in the transverse-field ising chain, Phys. Rev. B **106**, 125149 (2022).
[56] B. Bleaney and M. R. Wells, Radiofrequency studies of $TmVO_4$, Proceedings of the Royal Society of London. Series A, Mathematical and Physical Sciences **370**, 131 (1980).
[57] R. Feigelson, Flux growth of type RVO4 rare-earth vanadate crystals, J. Am. Ceram. Soc. **51**, 538 (1968).
[58] S. Smith and B. Wanklyn, Flux growth of rare earth vanadates and phosphates, J. Cryst. Growth **21**, 23 (1974).